Modification of Sn/S Cages with Bisfunctionalized Ferrocenyl Units

Zhiliang You, Dieter Fenske, Stefanie Dehnen*

Fachbereich Chemie, Philipps-Universität Marburg,
Hans-Meerwein-Straße, D-35043Marburg, Germany

email: dehnen@chemie.uni-marburg.de

SUPPORTING INFORMATION

1. Experimental Syntheses Details

***General*:** All reaction steps were carried out under Ar atmosphere. All solvents were dried and freshly distilled prior to use. Organotin sulfide clusters $[(R^{2,\,3}Sn)_4S_6]$ (R^2= $CMe_2CH_2C(Me)O$, R^3 = $CMe_2CH_2C(Me)=NNH_2$) and 1,1´-diformylferrocene fC[C(O)H]$_2$ were prepared according to the reported methods.[1][2] The synthesis of ferrcene-1,1´-dicaboxylic acid hydrazide fC[C(O)NH-NH$_2$]$_2$ was slightly modified (see below).[3] Oxalyl chloride ($C_2O_2Cl_2$) and hydrazine monohydrate 64-65% ($N_2H_4{\cdot}H_2O$) were purchased from Aldrich.

^{1}H NMR, ^{13}C NMR and ^{119}Sn NMR measurements were carried out using a Bruker DRX 400 MHz spectrometer at 25ºC. In ^{1}H and ^{13}C NMR, the chemical shifts were quoted in ppm relative to the residual protons of deuterated solvents. In ^{119}Sn NMR, Me_4Sn was used as internal standard.

Infrared (IR) spectra were recorded on a Bruker TENSOR 37 FT-IR-Spektrometer.

Mass spectrometry (MS) was performed on a Finnigan MAT 95S. The Electrospray Ionisation (ITMS-ESI) spectra were obtained by using solvent as the carrier gas.

UV/Vis spectra were recorded on a Perkin- Elmer Cary 5000 UV/Vis/NIR spectrometer in the range of 800–200 nm employing the double-beam technique. The samples were prepared as suspension in nujol oil between two quartz plates.

Synthesis of Ferrcen-1,1´-dicaboxylic acid hydrazine

A mixture of ferrocene dicarboxylic acid fC[COOH]$_2$ (0.424 g, 1.55 mmol) in dichloromethane (DCM, 15.0 mL) was cooled with an ice bath. Oxalyl chloride (5.00 mL, 59.1 mmol) was then slowly added and the reaction mixture was then heated under reflux for 3 h. After removing the solvent and excess oxalyl chloride under vacuum, the resulted carboxylic chloride was dissolved in THF (15.0 mL), and added dropwise to a solution of hydrazine monohydrate (5.00 mL, 105 mmol) in ethanol (15.0 mL). The mixture was then stirred for 3 h at room temperature and heated under reflux for 18 h. Dark insoluble decomposition products formed in the heat, which were removed by filtration. The filtrate was then evaporated in vacuo until a precipitate formed. The resulting yellow solid was washed several times with ethanol and dried in vacuo. Yield: 0.240 g, 51.3%.

MS (ESI): *m/z* = 303.1([M+H]$^+$), 325.1 ([M+Na]$^+$). Elemental analysis, calculated (%) for $C_{12}H_{14}N_4O_2Fe_1$: C 47.71, H 4.67, N 18.55; found: C 47.17, H 4.70, N 18.51.

Synthesis of $[(R^{fC1}Sn_2)_2S_6]\cdot 3CH_2Cl_2$, *{**1**·*$3CH_2Cl_2$, R^{fC1} = $[CMe_2CH_2C(Me){=}N{-}N{=}C(H)]_2fC]$*}*

fC[C(O)H]$_2$ (0.0097 g, 0.04 mmol) and $[(R^3Sn)_4S_6]$ (0.0224g, 0.02 mmol) were suspended in a solvent mixture of methanol (MeOH, 3 mL) and DCM (3 mL). The mixture was heated under reflux for 17.5 h and then filtered. The filtrate was layered with *n*-pentane (1:1). Red block-shape crystals of **1** were obtained within 3 weeks. Yield: 0.0171 g, 55.7% (calculated on basis of $[(R^3Sn)_4S_6]$)

^{1}**H** NMR (400 MHZ, CD_2Cl_2, 25°C): *δ/ppm* = 1.35, 1.52 (ss, 24H; ***Me***$_2$C), 2.09 (s, 12H; ***Me***), 2.58 (dd, 8H; C***H***$_2$), 4.30, 4.63, 4.79, 5.25 (4m, 4x4H; Cp-***H***), 9.55 (s, 4H, ***H***-C=N-); ^{13}**C** NMR (100 MHZ, CD_2Cl_2, 25°C): *δ/ppm* = 19.66 (N=C***C***H$_3$), 25.41, 25.99 ((***C***H$_3$)$_2$C), 36.03 (***C***Me$_2$), 50.87 (***C***H$_2$), 65.33, 70.19, 71.45, 76.04 (H***C***-Cp)), 79.98 (-***C***-Cp), 163.54 (Cp(H)***C***=N), 169.41 (Me(CH$_2$)***C***=N); ^{119}**Sn** NMR (149 MHz, CD_2Cl_2): *δ/ppm* = –64.6; MS (ESI): *m/z* = 1530.7 ([M+H]$^+$); IR cm^{-1}: 3078.17 (C-H of Cp), 1633.59, 1591.16 (C=N), 1139.85 (N-N). Elemental analysis, calculated (%) for $C_{49}H_{66}N_8Cl_2Fe_2S_6Sn_4$: C 36.40, H 4.13, N 6.93, S 11.90; found: C 36.75, H 4.24, N 6.84, S 11.47. Note that only two solvent molecules remained after the drying process in high vacuum for 6 hours prior to the analysis.

Synthesis of $[(R^{fC2}Sn_2)_2S_6]\cdot5CH_2Cl_2$, $\{\mathbf{2}\cdot5CH_2Cl_2$, $R^{fC2} = [CMe_2CH_2C(Me){=}N–NHC(O)]_2fC]\}$

$fC[C(O)NH\text{-}NH_2]_2$ (0.025 g, 0.083 mmol) and $[(R^2Sn)_4S_6]$ (0.044g, 0.0413 mmol) were suspended in a solvent mixture of MeOH (5.00 mL) and DCM (5.00 mL). The mixture was heated under reflux for 17.5 h. Dark insoluble decomposition products formed in the heat, which was removed by filtration. The filtrate was evaporated in vacuo. The resulting yellow solid was dissolved in DCM (6.00 mL), and layered with *n*-pentane (1:1). Orange block-shape crystals of **2** were obtained within 10 days. Yield: 0.0340 g, 51.6% (calculated on basis of $[(R^2Sn)_4S_6]$)

^{1}**H** NMR (400 MHZ, CD_2Cl_2, 25°C): *δ/ppm* = 1.35, 1.52 (ss, 24H; ***Me***$_2$C), 1.89 (s, 12H; ***Me***), 2.76 (dd, 8H; C***H***$_2$), 4.41, 4.55, 4.75, 5.43 (4m, 4x4H; Cp-***H***), 9.10 (s, 4H, ***H***-NC=O); ^{13}**C** NMR (100 MHZ, CD_2Cl_2, 25°C): *δ/ppm* = 21.85 (N=C***C***H$_3$), 26.74, 27.28 ((***C***H$_3$)$_2$C), 36.18 (***C***Me$_2$), 52.16 (***C***H$_2$), 68.11, 71.51, 73.30, 74.01 (H***C***-Cp)), 77.82 (-***C***-Cp), 165.48 (Cp***C***=O-NH), 173.29 (Me(CH$_2$)***C***=N); ^{119}**Sn** NMR (149 MHz, CD_2Cl_2): *δ/ppm* = –78.3; MS (ESI): *m/z* = 1618.8 ($[M+Na]^+$); IR cm^{-1}: 3313.47 (N-H), 3053.10 (C-H of Cp), 1685.67 (C=O), 1664.45 (C=N), 1168.78 (N-N). Elemental analysis, calculated (%) for $C_{49}H_{66}N_8O_4Cl_2Fe_2S_6Sn_4$: C 35.01, H 3.96, N 6.67, S 11.45; found: C 35.80, H 4.25, N 6.34, S 11.26. Note that only one solvent molecule remained after the drying process in high vacuum for 6 hours prior to the analysis.

2. Spectrometry and Spectroscopy

ESI mass spectra:

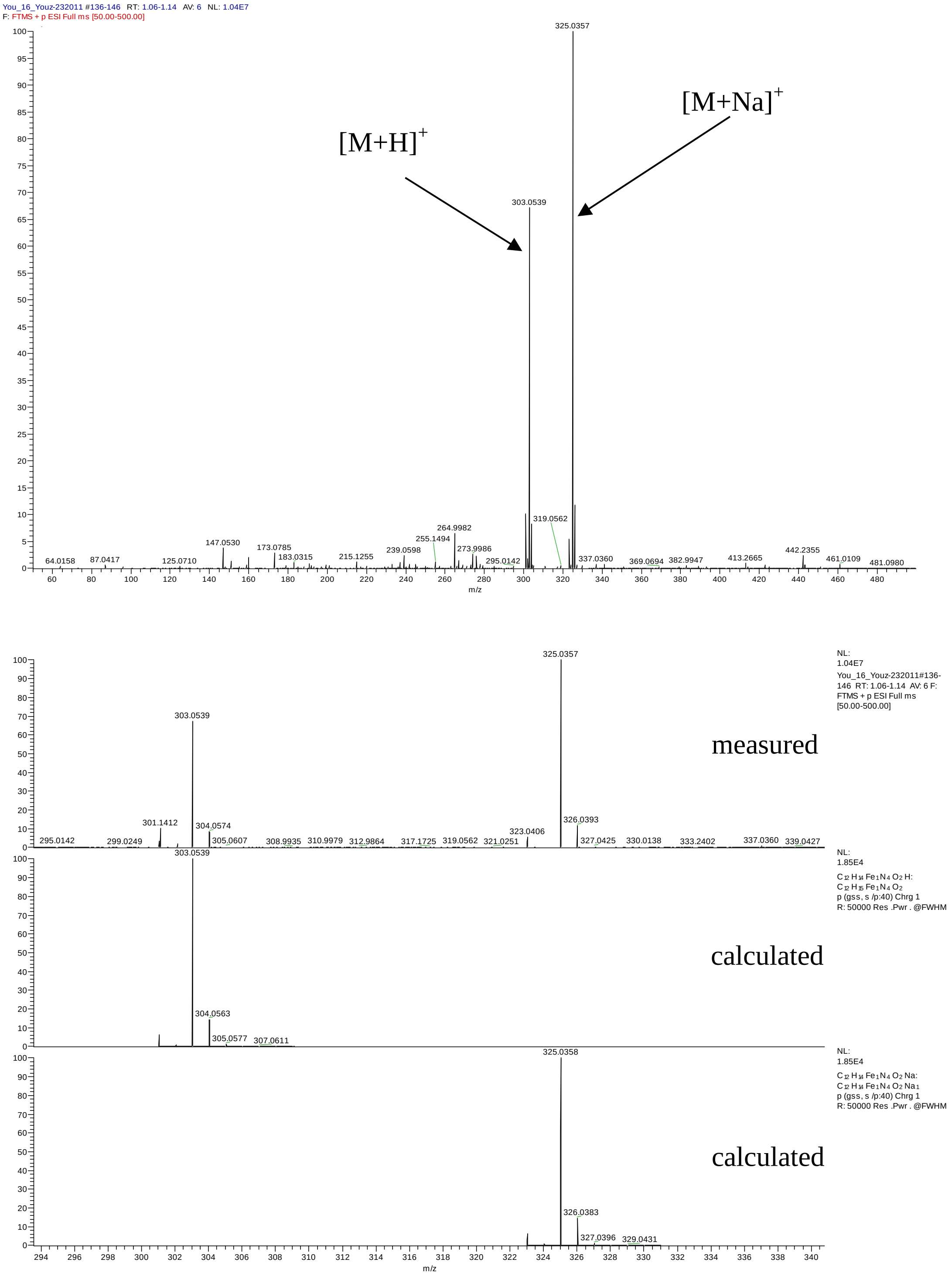

Figure S1. ESI mass spectrum of **fC[C(O)NH-NH$_2$]$_2$**.

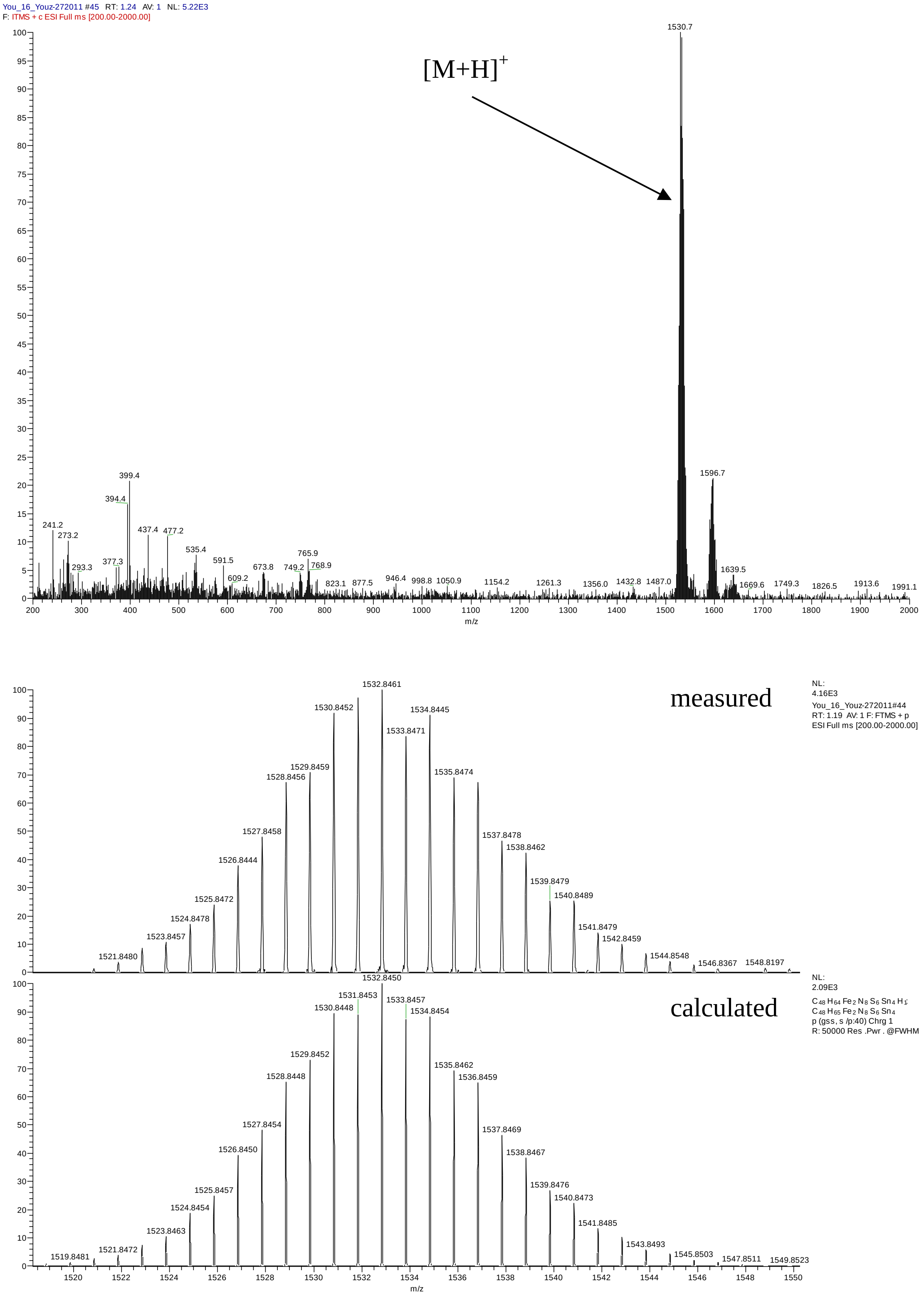

Figure S2. ESI mass spectrum of **1**.

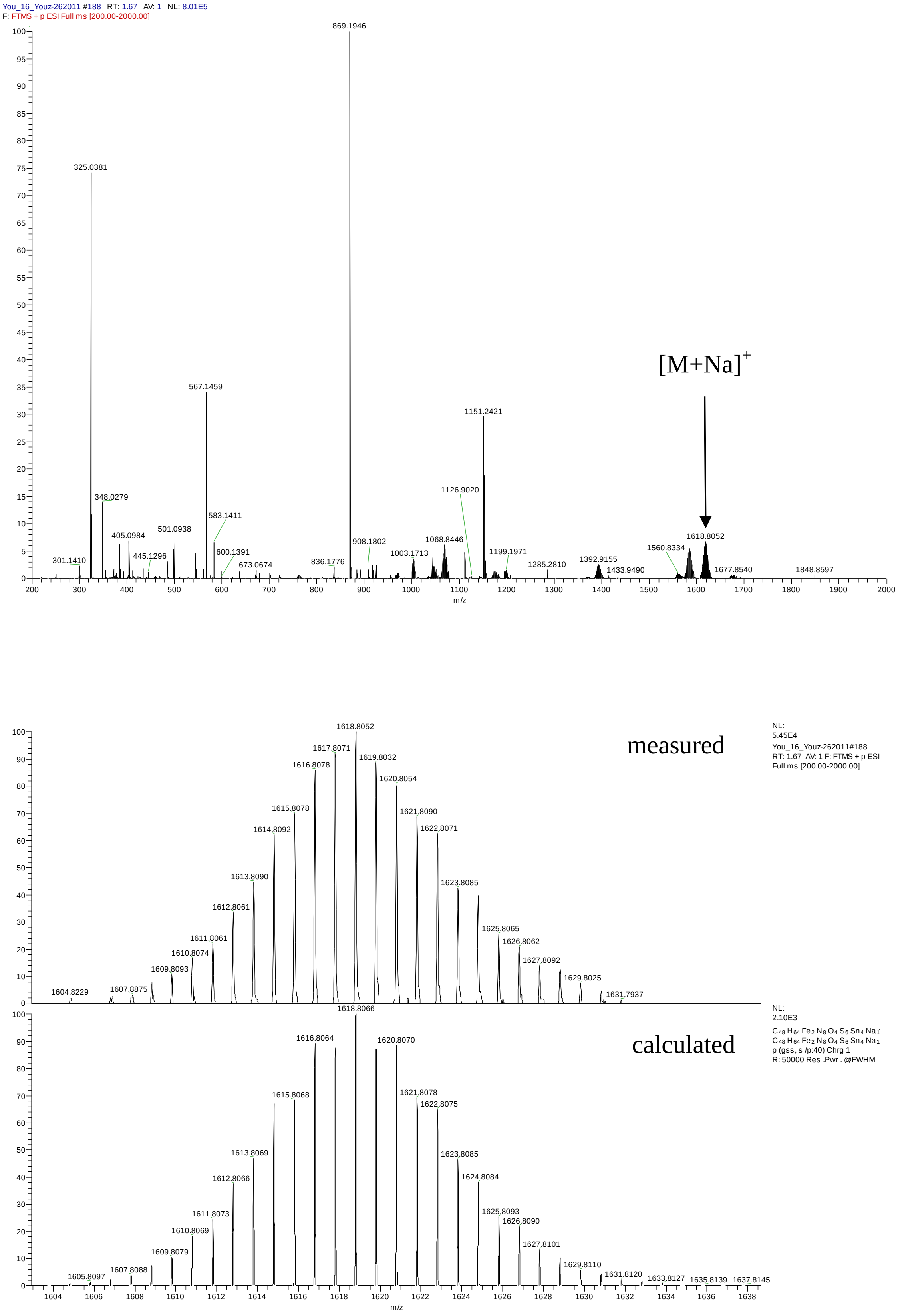

Figure S3. ESI mass spectrum of **2**.

Temperature-dependent ^{1}H NMR spectra of 2:

The conformational difference between the two ferrocene units in **2** (see molecular structure) is offset in solution. However, the structures with co-planar Cp rings and their binding chains (C=O double bond) are rigid, neither the Cp rings nor the attached organic chains can freely rotate. In such rigid conformation, the four protons of the same Cp ring are chemically non-equivalent. Hence, there are four separate signals. Additionally, one signal, which belongs to proton H9 (see figure S4), is shifted downfield due to the anisotropy that results in a closer proximity of the electron pair at the adjacent O atom.

In order to examine the potential influence of conformational changes at the spacers on the cage geometry, we carried out ^{1}H NMR measurements at different temperatures. For this, a solution of **2** in tetrachloroethan-d$_2$ was heated up to 370 K. The increased temperatures should result the increasing of the flexibility both of the Cp rings and the chains that attach them to the Sn/S cluster. As a result, the Sn/S cluster should become higher symmetric, leading to identical signals between chemical identical protons. In fact, no considerable changes were observed. We therefore conclude that the conformational peculiarities observed for **2** are not maintained in solution.

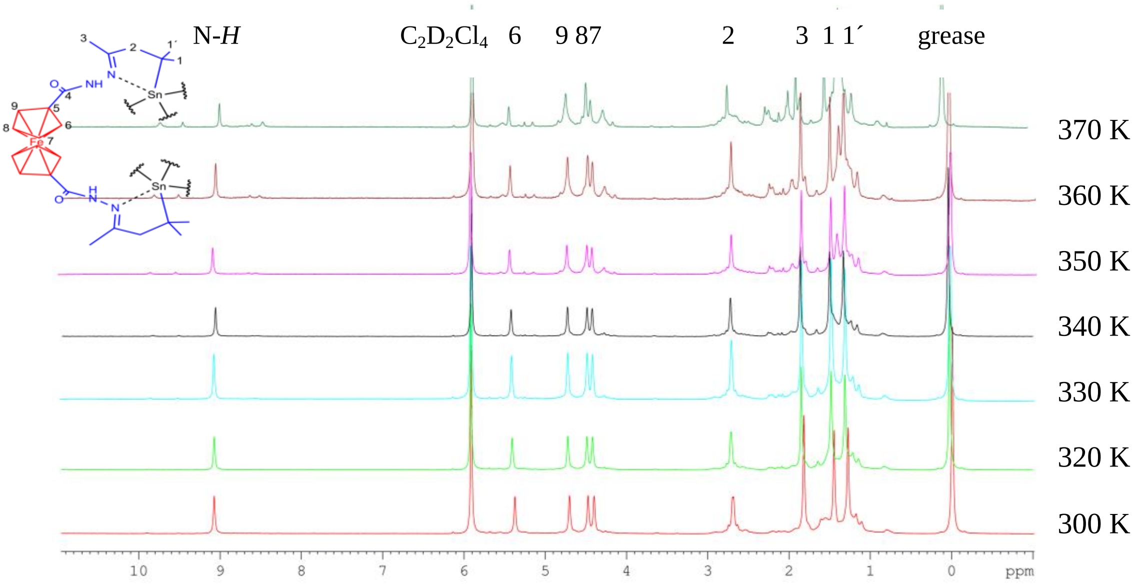

Figure S4. ^{1}H NMR spectra of **2** in tetrachloroethan-d$_2$ ($C_2D_2Cl_4$) with increasing measuring temperature (300 ~ 370 K).

UV-visible spectra:

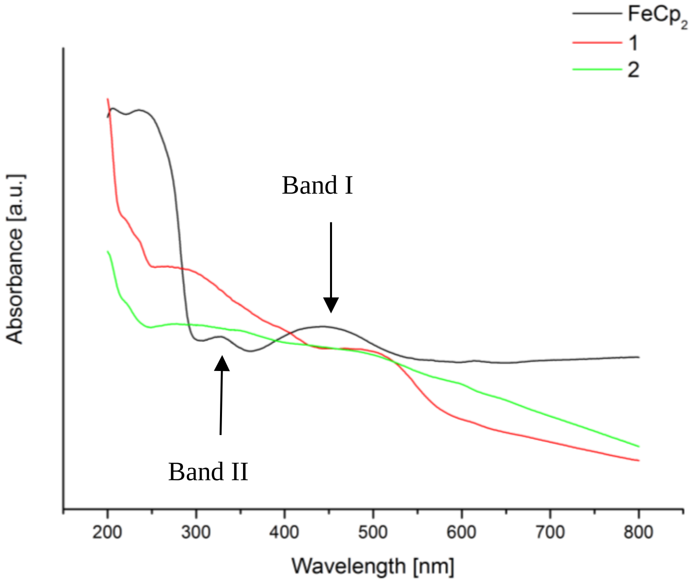

Figure. S**5** Solid-state UV-visible spectra of compounds **1** (red), **2** (green) and ferrocene (black), recorded as suspensions of single crystals in nujol oil.

The spectrum of ferrocene in the solid state displays two significant broad absorption bands, I at 445, and II at 328 nm, similar to the values recordred in ethanol solution (band I at 400, and II at 325 nm).[4]

Compound **1** has two distinct broad maxima at 514 and 270 nm, which can be assigned to the fC-containing organic spacer ($[CMe_2CH_2C(Me)=N–N=C(H)]_2fC$) and to a p(S)→p(Sn) charge transfer of the Sn-S-skeleton, respectively, according to similar reported values.[5,6] Compared with band I of pure ferrocene, the absorption band of the ferrocene units in **1** has a notable redshift of 69 nm, which is probably caused by the presence of the carbonyl substituent on ferrocene.[5] The according redshift of band I in compound **2** (about 55 nm) is smaller than observed for **1**. The absorption band at 273 nm can be also assigned to a p(S)→p(Sn) charge transfer. In both compounds, the second ferrocene-derived band II is observed, but the absorption is very weak, complicating an accurate estimate of their positions (ca. 401 nm in **1** and ca. 357 nm in **2**). For explanations, see the main manuscript text.

3. X-ray diffraction measurement, structure solution and refinement details

Data were collected on a diffractometer equipped with a STOE imaging plate detector system IPDS2T, using MoKa radiation with graphite monochromatization (λ = 0.71073 Å) at 100 K. The structure solution was performed by Sir-2004,[7] full-matrix-least-squares refinement against F^2, using SHELXS-97 and SHELXL-97 software.[8] Details of the data collections and refinements are given in Table S1. Selected bond lengths and bond angles are provided in Tables S2 and S3.

Table S1. Crystallographic and refinement details of **1** and **2**.

Compound	**1**·3CH$_2$Cl$_2$	**2**·5CH$_2$Cl$_2$
Chemical formula	$C_{51}H_{70}Cl_6Fe_2N_8S_6Sn_4$	$C_{53}H_{74}Cl_{10}Fe_2N_8O_4S_6Sn_4$
Formula Mass/g·mol^{-1}	1786.81	2020.52
Crystal color and shape	red block	orange block
Crystal size /mm^3	0.28×0.11×0.05	0.17×0.09×0.08
Crystal system	Orthorhombic	Monoclinic
a/Å	12.605	15.731
b/Å	25.646	24.753
c/Å	41.912	21.079
β/°	90.00	111.58
V/Å3	13548.9	7632.5
Space group	$P2_12_12_1$	$P2_1/c$
Z	8	4
Radiation type	Mo Kα	Mo Kα
Abs. coefficient, μ/mm^{-1}	2.330	2.219
Abs. correction type	numerical	numerical
min/max transmission	0.743/0.890	0.7042/0.8425
2θ range /deg	2.50-50.00	2.66-53.54
No. of reflections measured	77481	75937
No. of independent reflections	22698	16134
R_{int}	0.0315	0.1320
R_1 ($I > 2\sigma(I)$) / $wR(F^2)$ (all data)	0.0396/0.1081	0.0431/0.1058
Goodness of fit on F^2	1.036	0.816
Largest diff. peak/hole /e$^-$·Å^{-3}	1.233/-0.726	1.454/-1.231

Compound ***1***:

All non-H atoms were refined employing anisotropic displacement parameters. Disordered dichlormethane molecules were refined using PART and SAME constraints.

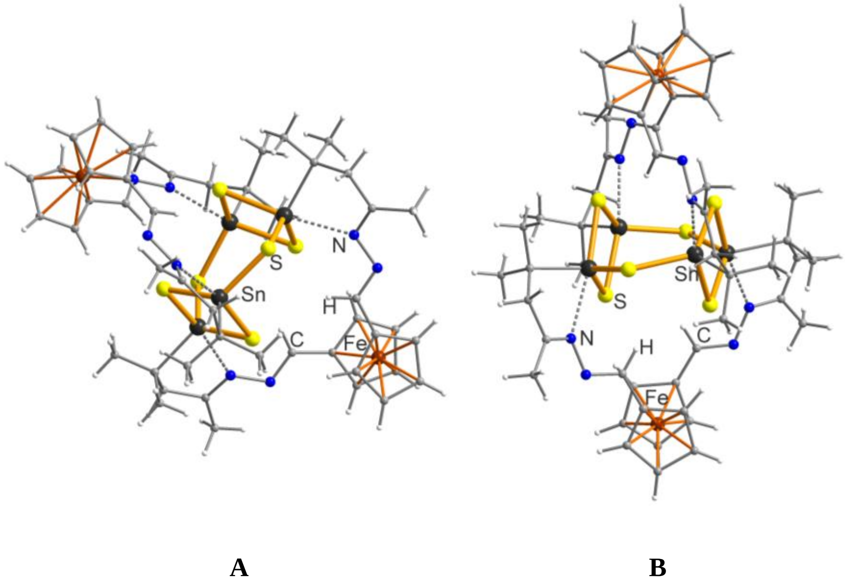

Figure S6. Molecular structures of the two independent molecules A (left) and B (right) in **1**.

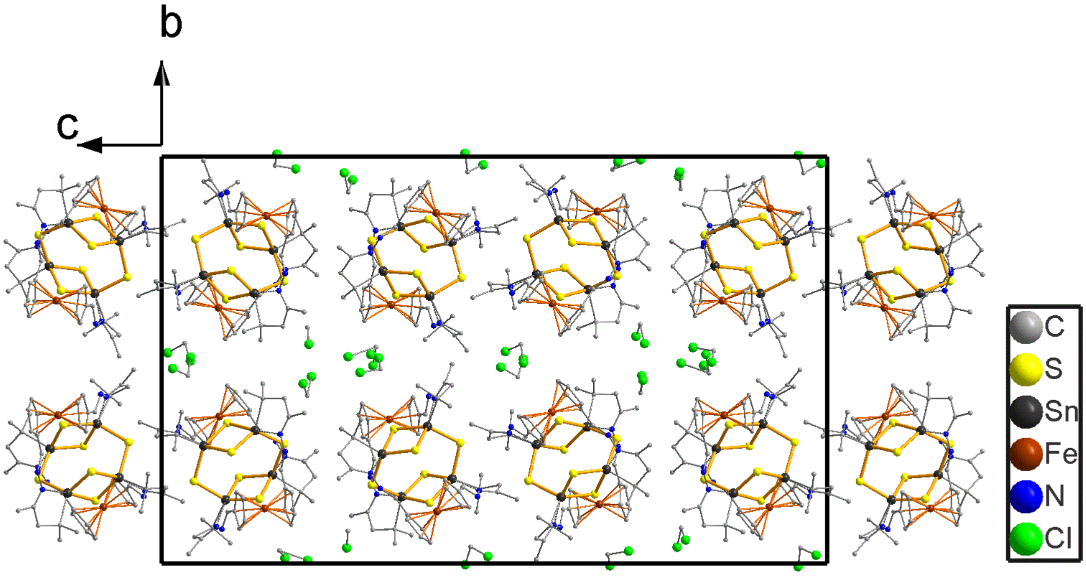

Figure S7. Packing of the molecules of $\mathbf{1}\cdot 3CH_2Cl_2$ in the crystal, viewed along the crystallographic *a* axis. H atoms are omitted for clarity.

Table S2. Selected bond lengths [pm], bond angles [°] in **1**·$3CH_2Cl_2$.

S(1)-Sn(1)	248.7(2)	Sn(2)-C(49)	218.8(8)
S(1)-Sn(2)	239.21(19)	Sn(3)-C(73)	216.6(8)
S(2)-Sn(1)	238.60(18)	Sn(4)-C(70)	219.8(8)
S(2)-Sn(2)	249.1(2)	Sn(5)-C(25)	217.4(7)
S(3)-Sn(3)	249.16(18)	Sn(6)-C(1)	217.8(8)
S(3)-Sn(4)	239.30(18)	Sn(7)-C(46)	220.7(7)
S(4)-Sn(3)	238.48(19)	Sn(8)-C(22)	218.7(7)
S(4)-Sn(4)	250.71(18)	Sn(1)-N(1)	253.8(9)
S(5)-Sn(1)	240.74(19)	Sn(2)-N(7)	246.9(8)
S(5)-Sn(4)	240.82(19)	Sn(3)-N(3)	254.7(6)
S(6)-Sn(3)	241.12(18)	Sn(4)-N(5)	248.3(6)
S(6)-Sn(2)	241.5(2)	Sn(5)-N(14)	250.2(6)
S(7)-Sn(6)	238.91(18)	Sn(6)-N(12)	253.1(5)
S(7)-Sn(5)	249.83(17)	Sn(7)-N(16)	248.8(6)
S(8)-Sn(5)	239.28(18)	Sn(8)-N(10)	250.7(6)
S(8)-Sn(6)	248.70(17)	Sn(2)-S(1)-Sn(1)	88.84(7)
S(9)-Sn(7)	249.6(2)	Sn(1)-S(2)-Sn(2)	88.89(7)
S(9)-Sn(8)	238.46(17)	Sn(4)-S(3)-Sn(3)	88.75(6)
S(10)-Sn(7)	239.08(17)	Sn(3)-S(4)-Sn(4)	88.57(6)
S(10)-Sn(8)	249.02(19)	Sn(1)-S(5)-Sn(4)	108.46(7)
S(11)-Sn(6)	242.29(18)	Sn(3)-S(6)-Sn(2)	109.74(7)
S(11)-Sn(7)	241.02(19)	Sn(6)-S(7)-Sn(5)	88.92(6)
S(12)-Sn(5)	241.0(2)	Sn(5)-S(8)-Sn(6)	89.10(6)
S(12)-Sn(8)	240.6(2)	Sn(8)-S(9)-Sn(7)	88.79(6)
Sn(1)-C(94)	217.6(9)	Sn(7)-S(10)-Sn(8)	88.79(6)

Compound ***2***:

All non-H atoms were refined employing anisotropic displacement parameters. An EADP constraint was used for the atom pair C49 C52. A disordered dichlormethane molecule was refined using PART and SAME constraints, and the C–Cl bond lengths were restrained to 1.76(2) Å with a DFIX restraint.

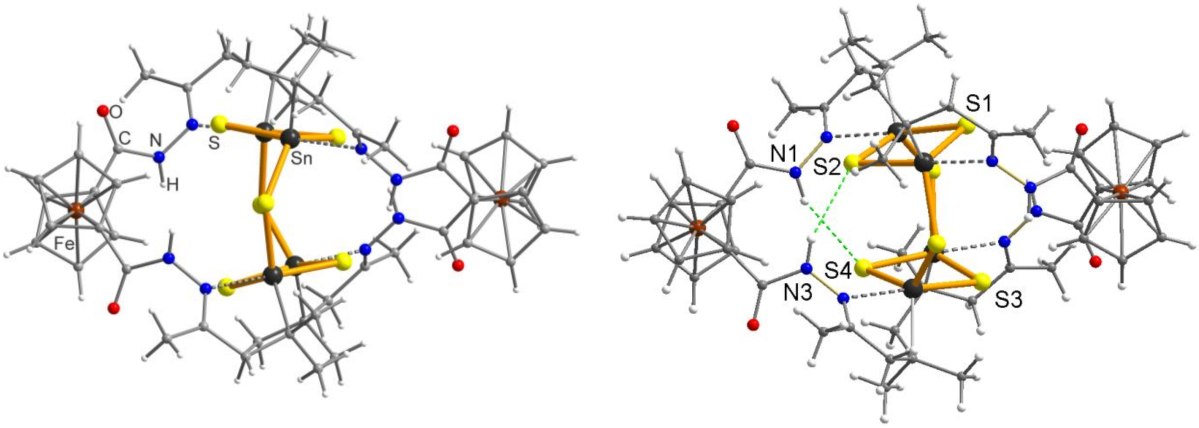

Figure S8. Molecular structure of **2** (left) and illustration of intramolecular hydrogen bonding (right).

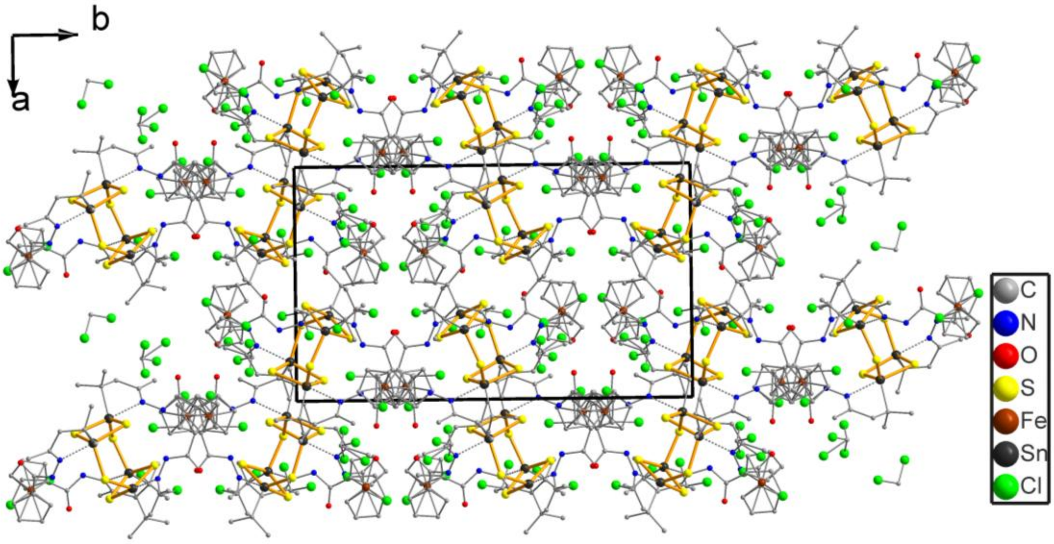

Figure S9. Packing of the molecules of **2**·5CH_2Cl_2 in the crystal, viewed along the crystallographic *c* axis. H atoms are omitted for clarity.

Table S3. Selected bond lengths [pm], bond angles [°] in **2**·5CH_2Cl_2.

S(1)-Sn(3)	239.3(2)	C(22)-Sn(2)	217.5(8)
S(1)-Sn(1)	248.25(19)	C(27)-Sn(1)	215.9(7)
S(2)-Sn(2)	238.91(19)	C(46)-Sn(4)	216.6(7)
S(2)-Sn(4)	249.1(2)	N(1)-Sn(3)	240.6(6)
S(3)-Sn(1)	241.5(2)	N(4)-Sn(2)	234.3(6)
S(3)-Sn(3)	249.59(19)	N(5)-Sn(1)	243.7(6)
S(4)-Sn(4)	241.32(19)	N(8)-Sn(4)	241.9(6)
S(4)-Sn(2)	248.5(2)	Sn(3)-S(1)-Sn(1)	88.09(6)
S(5)-Sn(2)	243.11(19)	Sn(2)-S(2)-Sn(4)	87.24(7)
S(5)-Sn(1)	243.6(2)	Sn(1)-S(3)-Sn(3)	87.29(6)
S(6)-Sn(3)	242.01(19)	Sn(4)-S(4)-Sn(2)	86.85(7)
S(6)-Sn(4)	242.8(2)	Sn(2)-S(5)-Sn(1)	111.92(8)
C(3)-Sn(3)	217.4(8)	Sn(3)-S(6)-Sn(4)	111.51(7)

4. Electrochemical measurements

All electrochemical measurements – cyclic and differential pulse voltammetry (CV and DPV) – were recorded under Ar atmosphere at 25 ^{o}C, using 0.1 mol/L [*n*-Bu_4N][PF_6] as the supporting electrolyte. The potentials were referenced internally to ferrocene, added at the end of the experiments. Working and counter electrodes: Pt; scan rate: 100 mV/s; pulse amplitude for DPV: 50 mV.

Table S4. Electrochemical characteristics for the oxidation process of the complexes **1** and **2** in DCM solution. (Measured at 100 mV/s, *vs.* [$FeCp_2$] in mV)

Complex	E_{pa}^{1}	E_{pa}^{2}	ΔE_{p}^{1}	ΔE_{p}^{2}	i_{pa}^{1}/i_{pc}^{1}	i_{pa}^{2}/i_{pc}^{2}
1	466	-	120	-	0.85	-
2	706	836	180	-	1.76	-

To investigate the electrochemical behavior of the double-decker cluster itself, we have performed a DVP analysis of the fC-free precursor [$(R^2Sn)_4S_6$] (Figure S10; R^2 = $CMe_2CH_2C(Me)O$). It indicates that the Sn/S framework itself is stable in the respective bias range.

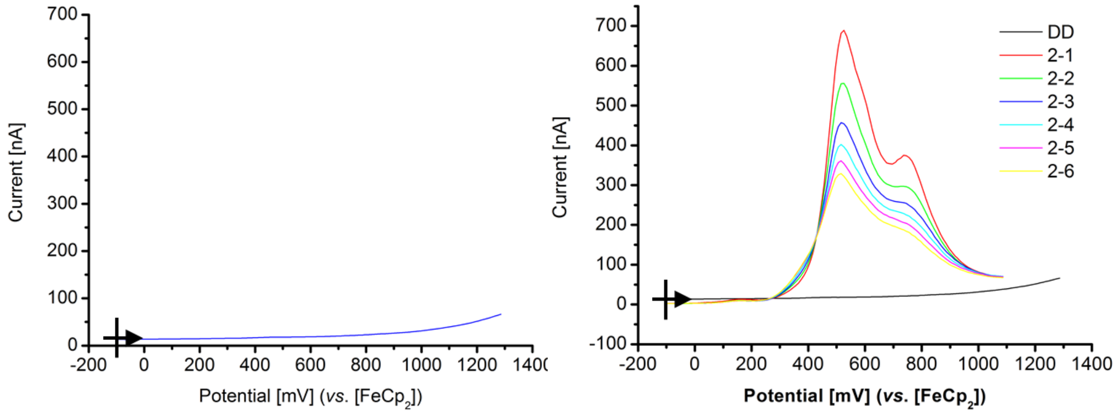

Figure S10. : DVP of $1.05 \cdot 10^{-3}$ mol/L of $[(R^2Sn)_4S_6]$ (“DD”, $R^2 = CMe_2CH_2C(Me)O$) in DCM along with 0.1 mol/L $[NBu_4][PF_6]$ (left), and comparison of the DVP of $[(R^2Sn)_4S_6]$ with that observed for **2** (right; see also Figure 2b in the main manuscript), in the range of –100 - 1300 mV, scan rate 10 mV/s, pulse amplitude 50 mV.

5. Quantum chemical analyses

Density functional theory (DFT) investigations were undertaken employing the program system TURBOMOLE (Version 6.2),[9] using the BP86 functional,[10] and def2-TZVP basis sets.[11] For Sn atoms, an effective core potential (ECP-28) was applied.[12] The molecules of **1** and **2** were investigated by simultaneous optimization of the electronic and geometric structures, starting out from the geometries observed experimentally in the crystal structures without application of symmetry restrictions (C_1 symmetry). Both molecules converged into near D_{2d} symmetric structures, thus the unsymmetric conformation of **2** did not turn out to be a systematic feature upon attachment of the very fC ligand, but to be due to secondary effects within the crystal structure.

6. References for the Supporting Information

[1] Z. H. Fard, L. Xiong, C. Müller, M. Hołynska, S. Dehnen, *Chem. Eur. J.* **2009**, *15*, 6595.

[2] A. Connell, P. J. Holliman, I. R. Butler, L. Male, S. J. Coles, P. N. Horton, M. B. Hursthouse, W. Clegg, L. Russo, *J. Organomet. Chem.* **2009**, *694*, 2020.

[3] Q. B. Song, Z. L. Lu, X. L. Wu, Y. X. Ma, *Transition Met. Chem.* **1994**, *19*, 503; S. Top, S. Masi, G. Jaouen, *Eur. J. Inorg. Chem.* **2002**, 1848.

[4] L. Kaplan, W. L. Kester, J. J. Katz, *J. Am. Chem. Soc.* **1952**, *74*, 5531.

[5] T. H. Barr, W. E. Watts, *J. Organomet. Chem.* **1968**, *15*, 177.

[6] Z. H. Fard, M. Hołynska, S. Dehnen, *Inorg. Chem.* **2010**, *49*, 5748.

[7] M. C. Burla, R. Caliandro, M. Camalli, B. Carrozzini, G. L. Cascarano, L. De Caro, C. Giacovazzo, G. Polidori, R. Spagna, *J. Appl. Crystallogr.* **2005**, *38*, 381.

[8] G. W. Sheldrick, Bruker AXS Inc., Madison WI, **1997**.

[9] TURBOMOLE GmbH **2011**. TURBOMOLE is a development of University of Karlsruhe and Forschungszentrum Karlsruhe 1989-2007, TURBOMOLE GmbH since 2007.

[10] A. D. Becke, *Phys. Rev. A* **1988,** *38*, 3098; J. P. Perdew, *Phys. Rev. B* **1996**, *33*, 8822.

[11] F. Weigend, R. Ahlrichs, *Phys. Chem. Chem. Phys.* **2005**, *7*, 3297, F. Weigend, *Phys. Chem. Chem. Phys.* **2006**, *8*, 1057.

[12] H. Stoll, B. Metz, M. Dolg, *J. Comput. Chem.* **2002**, *23*, 767.